 SDHM, vol.8, no.2, pp.91-109, 2012

Cumulative Damage by Miner's Rule and by Energetic Analisys

A. Risitano[1], D. Corallo[1] and G. Risitano[2]

Abstract: According to Miner's rule, the fatigue life of a material (or a mechanical component) is not a function of the order of the application of load. Many authors have already observed that the model proposed by Palmgren/Miner leads to underestimation of the damage and one of the reasons could be the disregard of the sequence of loads. Referring to the energy loss related to irreversible damage of the material, it was observed that the Miner's rule gives exact results only if the damage caused by the fatiguing load is low compared to the limit energy of the material. Whereas, if the damage caused by the fatiguing load is high, Miner's rule is no longer valid.

In this work, according to previous observations reported in other authors' works, tensile fatigue tests on AISI304 steel specimens were performed.

The load stories consisted of loading ramps in subsequent blocks. For each group of specimens the same blocks were applied but with inverted sequence. The surface temperature, recorded during application of loads, has been chosen as a benchmark of the damage.

Keywords: Rule of Miner, thermography, fatiguing loads

1 Introduction

One of the simplest assumptions for the assessment of the damage produced by fatiguing loads in the case of fatigue for high number of cycles is the one proposed by Palmgren-Miner (Miner's Rule) [Palmgren (1924); Miner (1945)]. Miner's rule is still the most widely used, mainly for its ease of application; indeed, for the estimation of the damage, it does not need factors depending on material characteristics. It is a well known fact, the law of Palmgren-Miner, in its original version, defines the damage produced on a generic material as the fraction of spent life (in terms of energy) for the particular load level.

[1] Catania University, Department of Industrial Engineering and Mechanics, Catania, Italy
[2] Guglielmo Marconi University, Faculty of Applied Science and Technology, Roma, Italy

According to this hypothesis, the rupture occurs when the sum of fractions of damage, defined only by the consumed cycles (n_i/N_i), at various load levels, reaches unity. It is synthesized by the simple relationship:

$$r = \sum_i \frac{n_i}{N_i} = 1 \tag{1}$$

where r is the factor of damage.

The last equation showing that does not exist any parameter function of the real energy, which, however, appears in the original hypothesis. It seems, then, that the same load applied at different moments in the life of the specimen or mechanical component produces the same damage, and even the load sequence has no effect for material life. In engineering literature however it is reported by several authors that the sum of the fractions of damage "r" to the break is not always equal to unity, but on the contrary, depends strongly on the sequence of applied loads. In particular, it was seen that "r" is greater than the unit when the sequence changes from low to high loads; on the contrary it is less than unity when the sequence goes from high to low loads. Iqbal Rasool Memon, Xing Zhang and Deyu Cui, (2002), for example, using sets of load, with different sequences between the yield stress of the material, they noticed that the Miner rule was valid only when the maximum values of the loads of the applied set were below the yield stress of the material.

In literature there are many models proposed by researchers [Corten and Dolan (1956); Haibach; Manson, Frecke and Ensign (1967); Singh (2001) and (2002)] based on assumptions of bilinear damage with double slope curves of fatigue.

These models, however, being based on the use of coefficients dependent on physical and mechanical properties of the material, lose the simplicity that characterizes the Miner rule in its application.

In literature there are also energy models (eg the work of Lefebvre and Ellyin) However, these models are never direct, ie, they always need coefficients characterizing the material, for their application.

To get an idea of the problem, in the work of Fatemi [Fatemi and Yang (1998)] in which he does a state of the art of the many methods (over 50) proposed to assess, more appropriately than Miner suggested, the damage and the resulting residual life of a mechanical component.

In previous works of writers [Risitano A. and Risitano G. *FIS* (2010)], it was highlighted as a model of linear damage proposed by Palmgren-Miner, once defined the fatigue limit, it was eligible to represent the remaining life of the material. In [Risitano A. and Risitano G. *JTAFM* (2010)], the writers, starting from the studies of the research team of Machine Construction of Catania [Curti, La Rosa, Orlando

and Risitano (1986); La Rosa and Risitano (2000); Fargione, Geraci, La Rosa and Risitano (2002)] in relation to the rapid estimation of the entire Wöhler curve, they showed, that the fatigue limit of damaged specimens could not only be characterized by the applied load history, but also by the sequence of loads. They also highlight how the energy parameter, $\Phi=\int \Delta T dn$ (integral of the surface temperature of specimen over time, until the break) represents in an appropriate way the limit energy to the break (E_l). In this way it was emphasized how the surface temperature of the specimen under fatigue loading, being a parameter function of the energy of plastic deformation (irreversible), was suited to represent the history of damage and the status of the material. In [Risitano A. and Risitano G. (2011)], it was underlined as for steels (materials considered homogeneous), a parameter of energetic damage $r_E = \Sigma \Delta T_i x n_i / \Phi$ in which the surface temperature appears can take into account, better than the parameter "r_M" of Miner (or other parameters in the various proposed models of damage), the energy consumed and the sequence of applied loads. Regarding the need of energy parameters for defining the state of the material and any eventual damage, we can find confirmation in the works of Atzori, Meneghetti and Ricotta (2009) and Naderi, Amiri and Khonsari (2009).

In this work, based on fatigue tests with a series of subsequent loads, performed on specimens of AISI 304 steel, an assessment of the surface temperature of the specimen is made, noting that the value ΔT for the damaged specimens not only depends on the history of applied load, but also by the sequence of load. Therefore, an assessment of the damage considering the parameter (ΔT) would lead to different results [Risitano A. and Risitano G. (2011)] from those that occur with the simple application of Miner's law, due to its formulation, cannot take into account the sequence at issue.

2 Comments on thermographic methodology

Before moving on to the description of the fatigue tests conducted, it is useful to summarize the results

obtained from A. Risitano and his collaborators since 1983 through the analysis of temperature on the surface of the specimen during the application of fatigue loading, by means of infrared heat sensors (full field). They can be summarized as follows:

- only when the stress $\Delta\sigma$ applied to the sample is higher than the fatigue limit $\Delta\sigma_0$, there is a temperature change ΔT above the initial temperature in some parts of the surface of the element under test;

- the temperature variation for internal damping of the totally elastic phase is

negligible compared to the temperature variation produced by irreversible micro-plasticity phenomena;

- for stress values below the fatigue limit the temperature variation $\Delta T2$ (stabilization temperature) is nearly 0 (Figure 1);
- for stress values higher than the fatigue limit, the temperature variation ΔT grows in the initial phase (about 10% of the number of cycles to break N) and then stabilizes at $\Delta T2$ almost to the stage of material failure (Figure 1);
- the slope of the temperature ΔT of the first phase is much "steeper", the higher the applied solicitation $\Delta\sigma$ is, compared to the fatigue limit $\Delta\sigma_0$;
- the temperature of stabilization $\Delta T2$ varies with the stress and it is much higher, the higher the applied solicitation $\Delta\sigma$ is, compared to the fatigue limit $\Delta\sigma_0$ (Figure 1);
- Loading a specimen (mechanical component) at equal test frequency, the integral of the temperature change ΔT is a constant of the material, such as the limit energy E_l is a constant of the material;
- Elementary energy per unit of volume spent after n_i cycles of application of the solicitation $\Delta\sigma$ over the fatigue limit $\Delta\sigma_0$, can be expressed as $\Phi_i g \approx \Sigma_i n_i \Delta T2_i$.

The observation 7, experimentally shown for the first time by Fargione, Geraci, La Rosa and Risitano (2002), is important for the assessment of the whole fatigue curve, and point 8 allows the spent energy ($\Phi_i \approx \Sigma_i n_i \Delta T2_i$.) after a determined number of cycles n_i to be evaluated different from Miner's formulation ($\Phi_i \approx \Sigma_i n_i$), but still easy to evaluate.

3 Materials and methods

The fatigue tests were conducted on six steel specimens AISI 304 with rectangular (Figure 2) using a load ratio R = - 1 and a frequency of 5 Hz. Table 1 and table 2 report the chemical and mechanical characteristics of the steel. Two different types of tests were identified (Figure 3): one with increasing and then decreasing load step called type A and another with decreasing and then increasing load step, called Type V (Table 3 and Figure 3). Each step is realized with 5000 cycles. The machine used for fatigue tests was the Instron 850 with load cell of 100 kN. The surface temperature of the specimen was detected by the thermograph flir SC3000 with an accuracy of 0.02 ˚C. Prior to the tests, the samples Were coated in black paint with emissivity at 0.9,

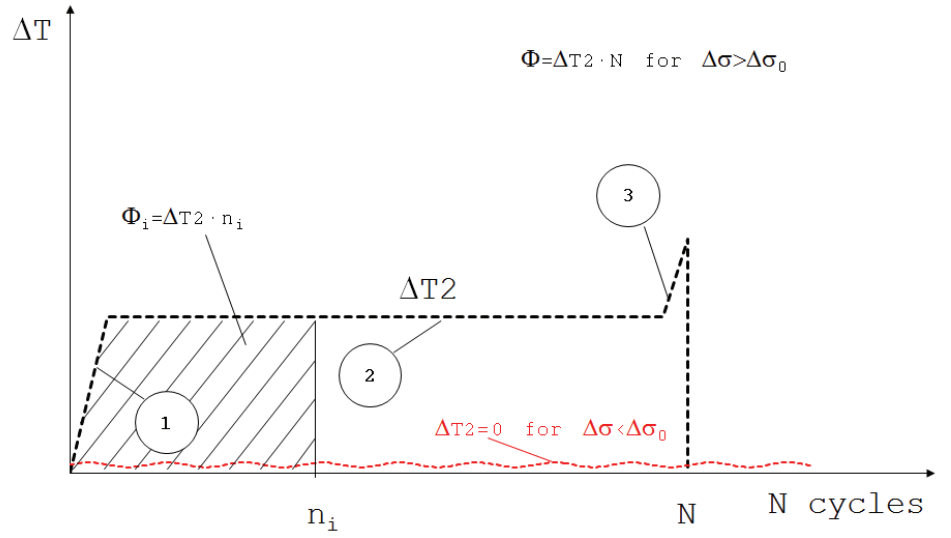

Figure 1: Generic evolution of temperature in function of the number of cycles during a monoaxial fatigue test with constant load.

Table 1: Chemical composition (in mass%).

	C	**P**	**S**	**Mn**	**Si**	**Cr**	**Ni**
AISI 304 L	0,08	0,04	0,03	2	0,75	18	8

Table 2: Mechanical properties.

Tensile strength (annealed)	586	MPa
Yield strength (annealed)	241	MPa
Elongation (annealed)	55	%
Hardness (annealed)	80	RB
Elastic Modulus	193	GPa

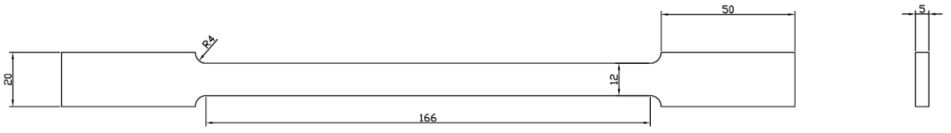

Figure 2: Used specimen sizes [mm].

Table 3: Typology of test for each specimen and its acronym.

Name	Type	Designation
Specimen 1	SP 01	A
Specimen 2	SP 02	V
Specimen 3	SP 03	A
Specimen 4	SP 04	V
Specimen 5	SP 05	A
Specimen 6	SP 06	V

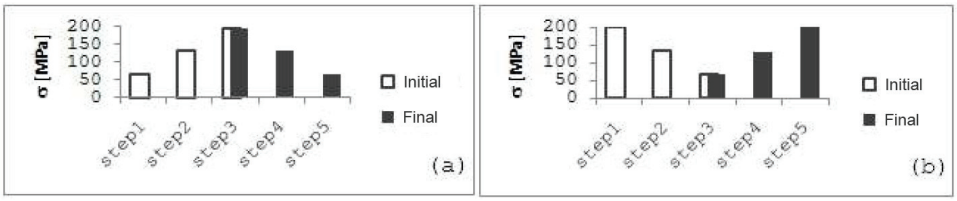

Figure 3: Value of the stress step for test type A (a) and V (b).

For each specimen and for each different stress level of each set (Figure 4) the surface temperature for the most stressed area during the test was detected. At the end of the application of each load step, the specimen was cooled to room temperature. No sample was led to breakup.

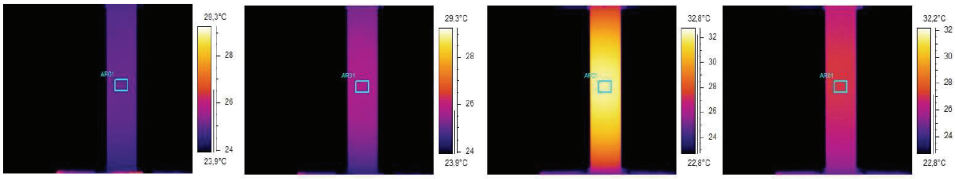

Figure 4: Thermographic images and survey area for one of the samples under test.

For the area under examination of each sample, the evolution of the temperature minimum, average and maximum was acquired (Figure 5). For the purpose of this study, we referred only to the maximum temperature T_{max} recorded (Figure 6) and in the diagrams was reported the difference of temperature ΔT between that value and the initial temperature of the sample (almost the same as room temperature).

For each specimen the stabilization temperature $\Delta T2$ reached at the end of each step was monitored (Figure 7). As proposed in previous papers, being linear the

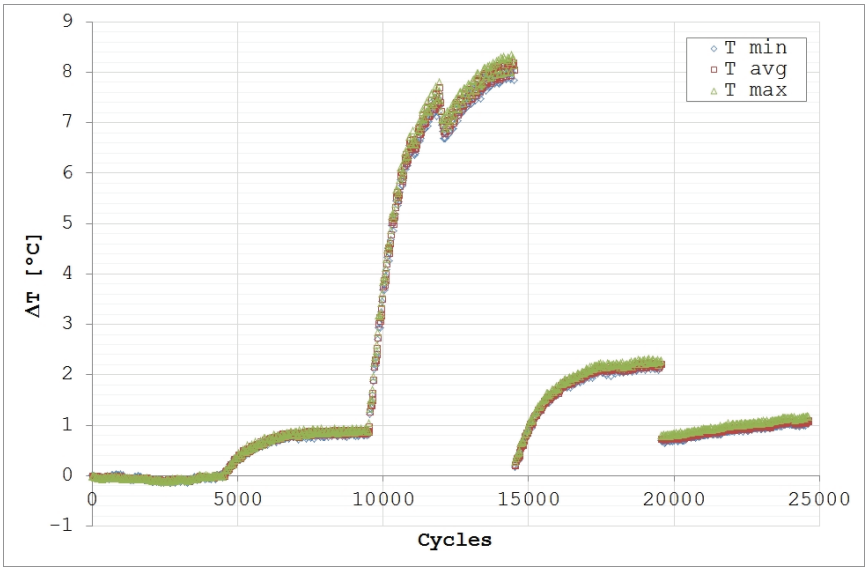

Figure 5: Trend of temperature difference minimums, averages and maximums depending on number of cycles for specimen SP 01 (type of test A).

relationship between the stabilization temperature $\Delta T2$ (Figure 1) and square of the nominal stress σ^2 [Fargione, Geraci, La Rosa and Risitano (2002)], the trend of this parameter for the first flight and for the second flight could be represented (Figure 8). As an example, the graphs relating to sample 01 SP are shown.

4 Results and discussions

Figure 9 shows the trends of the maximum temperature difference for the three samples (SP 01, SP 03, SP05) that were loaded with type A set of load (Tab.3), where the first ramp is a rise ramp (Figure3a) and second ramp is a drop ramp (Figure3b). Figure 10 shows the average trend of the three highest thermal increases for the three specimens. It is important to point out how, for each specimen (observable also in the average curve of the temperatures for the three samples in Figure 10), the stabilization temperatures ($\Delta T2$) in step 2 and in step 4 are very different, although the load level is the same. The same observation is valid for step 1 (practically 0, being with the first load level below the fatigue limit) and for the step 5 (the same load but with specimen already damaged due to the applied history of load). It is clear how step 3 (194 MPa), with a load exceeding the fatigue limit (in literature for these materials the fatigue limit is between 120 MPa and 140 MPa [Di Schino and Kenny (2003)]), has obviously damaged the specimen making it reach, in step

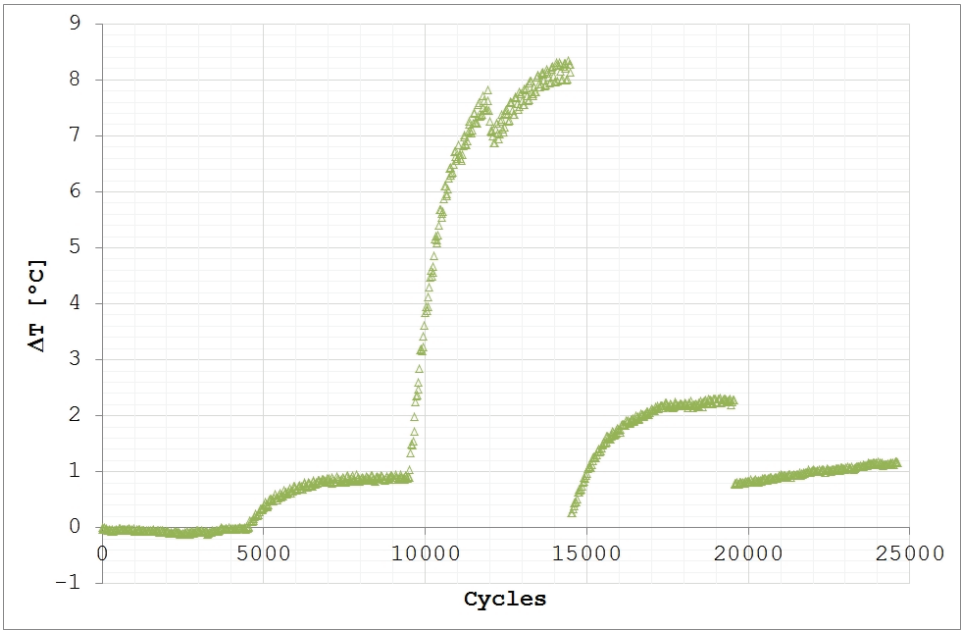

Figure 6: Trend of maximum temperature difference depending on number of cycles for specimen SP 01 (type of test A).

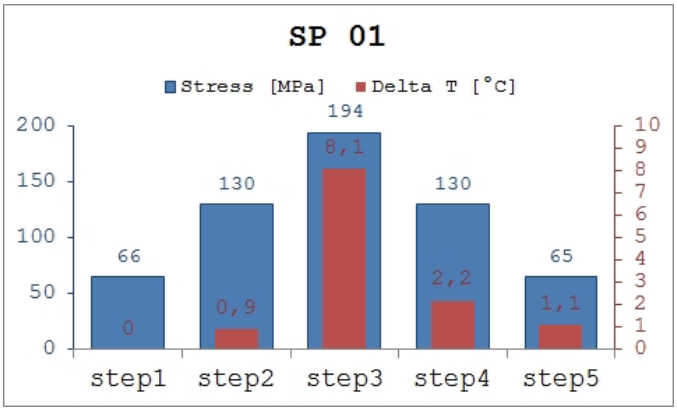

Figure 7: Value of temperature drop relative to the stabilization temperature for each step of specimen SP 01 (type of test A).

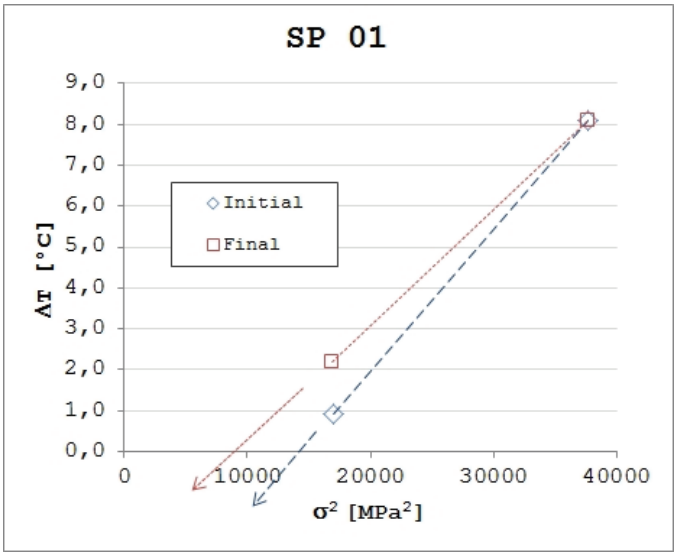

Figure 8: Trend for the rising ramp (blue diamond) and the drop ramp (red square) of the thermal jump relating to the stabilization temperature with the square of the stress for specimen SP 01 (type of test A).

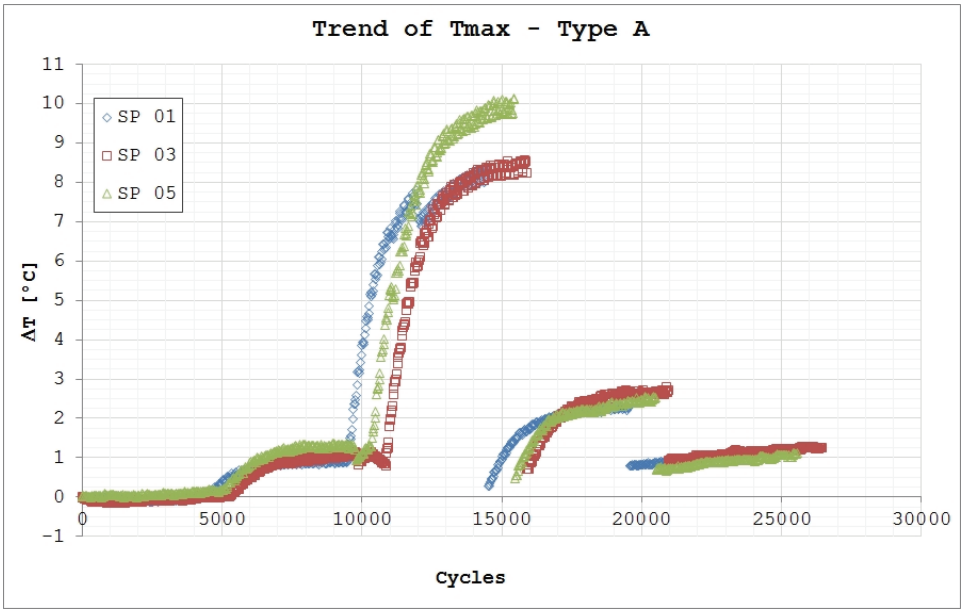

Figure 9: Evolution of temperature drop in function of number of cycles for the three specimens subjected to type A test.

4, a value of the stabilization temperature more than one degree higher than that found in step 2 even if the applied load value is the same.

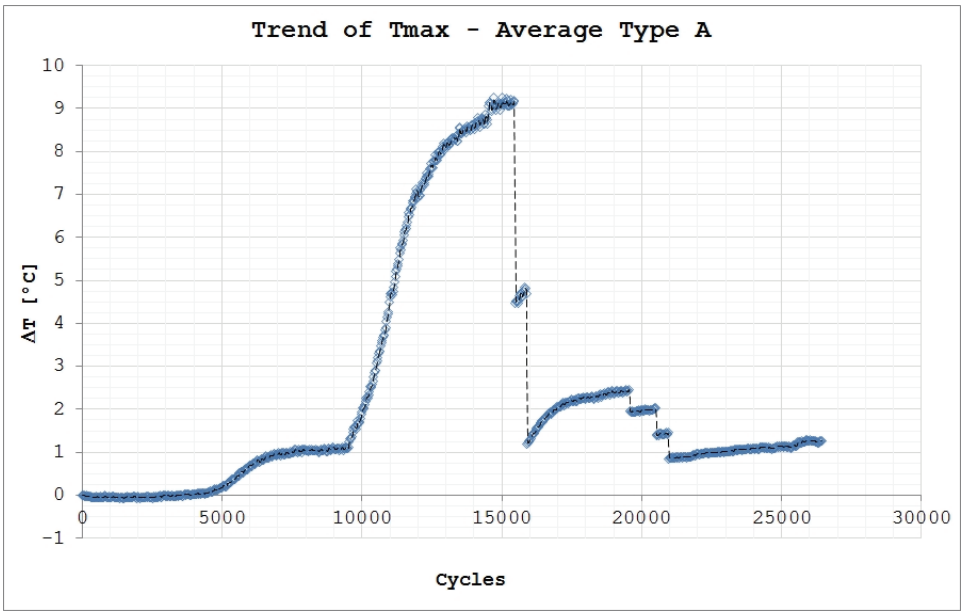

Figure 10: Trend of averaged curve of temperature difference in function of number of cycles for the three specimens subjected to type A test.

In Figure 11 similarly to what was done for the previous specimens, the trends of the maximum thermal jumps for the other three specimens (SP 02, SP 04, SP06) loaded with a type V load set (Table 3) are shown, ie first ramp descending, second ramp rising (Figure 3b). The average trend for the three maximum thermal jumps is shown in Figure 12. The observations for type A set are the same as type V. For each sample, the stabilization temperature of the first ramp steps are different from those of the second ramp.

Referring to the average curve of Figure 12, we can note that for the same applied load, the thermal jumps of the second ramp are always greater. Even for the lower load (lower than the fatigue limit) we can see an increase in temperature respect at room temperature (ΔT). This is a sign of damage caused by the ramp loads (descending) . The temperatures between step 2 and step 4 differ by 0.6 $^{\circ}$ C; the temperature between step 1 and step 5 differ by more than 1 $^{\circ}$C.

In Figure 13 the average trends between the maximum temperature differences (already represented in Figure 9 and 11) for the load types A and V are compared.

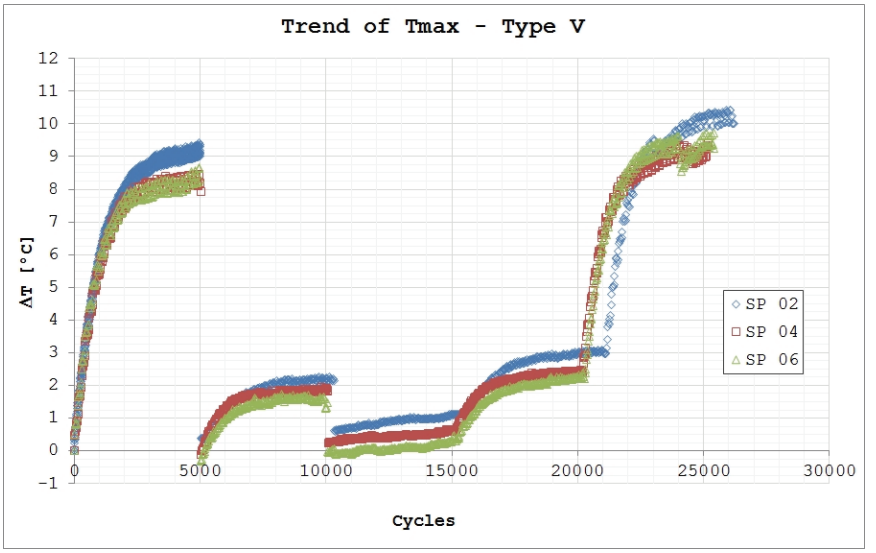

Figure 11: Evolution of temperature drop in function of the number of cycles for the three specimens subjected to type V of test.

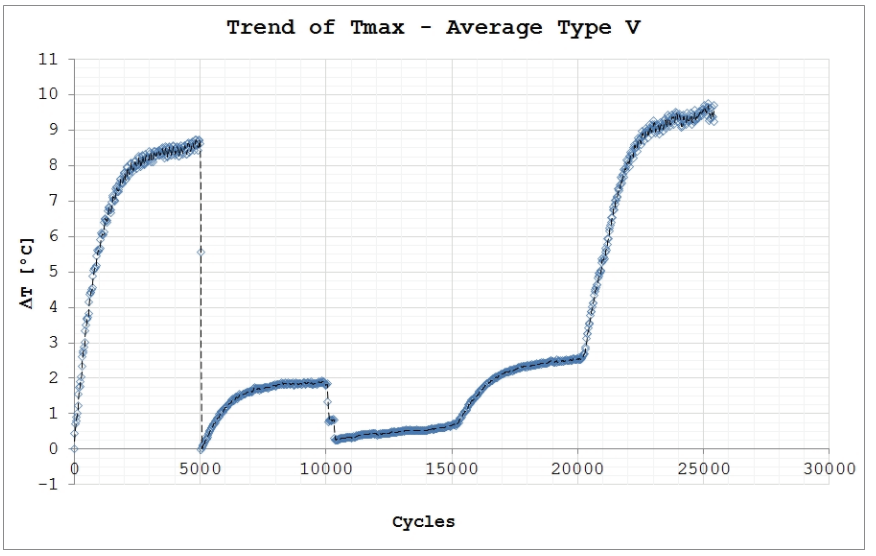

Figure 12: Trend of the averaged curve of temperature difference in function of the number of the cycles for the three specimens subjected to type V test.

It is interesting to note what happens in step 2 of the first and second ramps. The stressed specimens with V-type loading in the first ramp have a temperature significantly higher respect in type A. This is in line with the fact that in the second load step the specimen is damaged by the V type ramp, whereas it is still virtually intact if charged by type A. Comparing what is always happening in the same step of the second ramp, we notice that, in this case, the relative temperature of stabilization is practically the same (less than 0.5°C). In fact, in that state, the load history, in terms of damage, is almost the same as showed in table 4 (r_E=15,77x$10^{-2}$for Type A and r_E=19,83x10^{-2} for type V). In Figure 14 the curves of the average temperature of the three specimens for the first ramp are shown (first part of Figure 13). They show in a more direct way the thermal response for undamaged specimens subjected to equal loads but with different sequences (first increasing loads and then decreasing loads). It is clear how, for the same load, for the two different sequences, the temperatures are different. As noted above, the assessment of the damage, taking into account the temperature parameter, working as in [Risitano A. and Risitano G. (2011)], would lead to values of damage different from those calculated using the formulation of Miner. Proceeding, as shown in Figure 8, even with the temperature curves in function of the square of the applied stress, the values of the trend of the fatigue limit are lower depending on the damage (moved curves). For example, in Figure 15 and 16 only the trend obtained with the values of the average temperatures of the three specimens for the two load types A and V are shown.

To evaluate the damage at the different levels in the two load types (A,V), visible in Figure 13 and 14 as different value of temperature for equal load, the fatigue curve by Risitano's method was performed.

According to the method, in Figure 17 is reported the average temperatures vs number of cycles for three specimens loaded at different level (f=5 Hz). For each step, the stress changed after 5000 cycles. Also the levels of the stress are indicated in Figure 17. The maxima difference in temperature registered for the tree specimens was less than 0,2 °C. All the specimens were loaded until the failure. With the data recorded the fatigue limit resulted 120 N/mm^2 (Figure 18) and the parameter $\Phi = \Delta T\, dN$ calculated from the area under the line shown in figure 17, for the total number of cycles to failure (46000), was evaluated as 325000 [°C x Cycles]. According to the method, known the temperature of stabilization for each load, being Φ constant independently from the load history applied to the specimen, as possible to determine the Wohler's curve as in Figure 19 where the found points are reported as circles. In the same figure the experimental data points, coming from traditional method, for AISI with equal mechanical characteristics, found in literature [Di Schino and Kenny (2003)] are reported as x. In the figure 19 the strait line linking the limit fatigue point (2x10^6, σ_0) to the yield point (0, $\sigma_{0.2}$) is reported

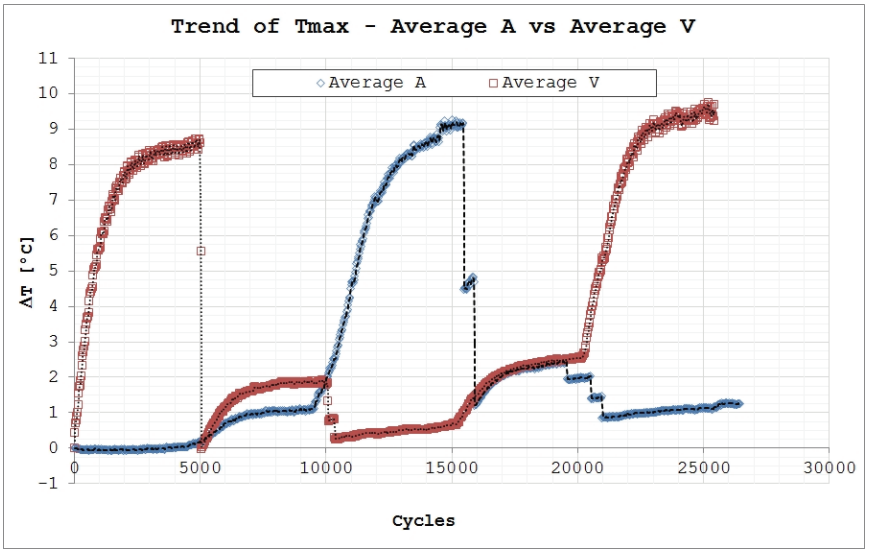

Figure 13: Comparison of the average curves of temperature difference for A and V type test.

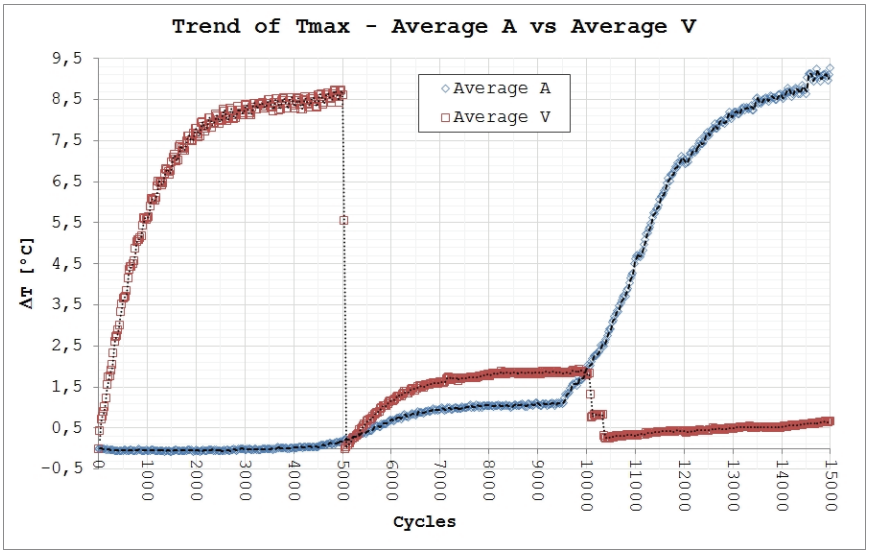

Figure 14: Detail (first three load steps) of Figure 3.a.

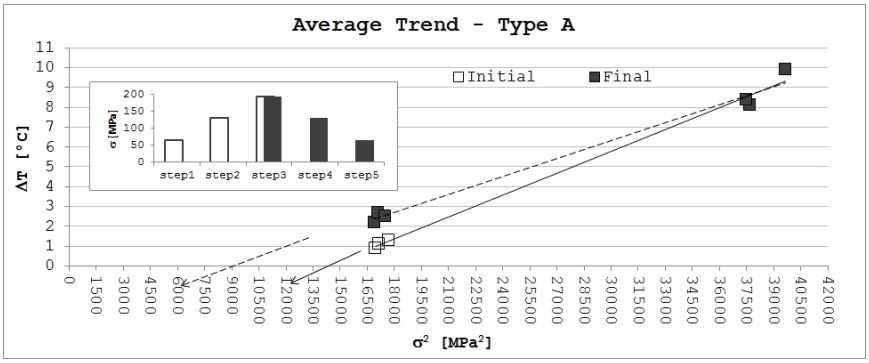

Figure 15: Average trend of temperature difference for type A test of the initial and final stroke in function of the square of the applied stress.

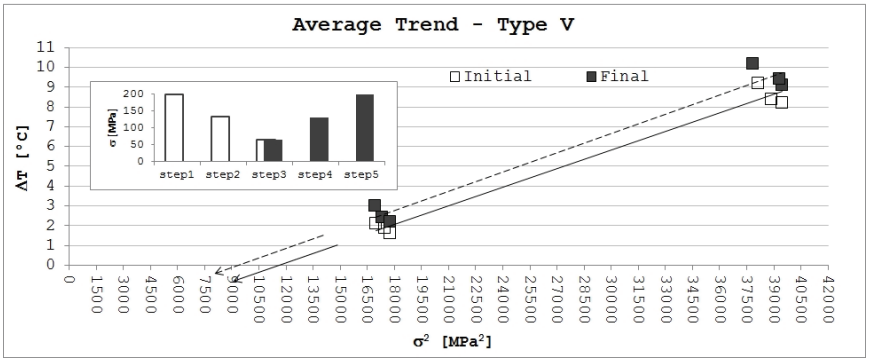

Figure 16: Average trend of the temperature difference for V type test of the initial and final stroke in function of the square of the applied stress.

also.

In table 4, for the two types of load sequence (A and V) and the equal applied stress (Figure20a and 20b), the values of the damage calculated by the Miner's rule (r_M) and by the energy loosed (r_E) for equal cycles number and equal applied loads, were reported. The ratio damage r_E was calculated as ratio between energetic parameters. Particularly as $\int \Delta T \, dn$ for the each applied load of the sequence (A and V) to the energetic parameter of the material Φ(5°C x Cycles). The analysis of the values of the table, show as for the two load sequence (A and V), the Miner's damage is the same and it is not dependent from the sequence of the loads (equal partial values and equal total value). In the contrary, the values calculated from a parameter of the energy loosed (r_E) are different for the partial values and for the

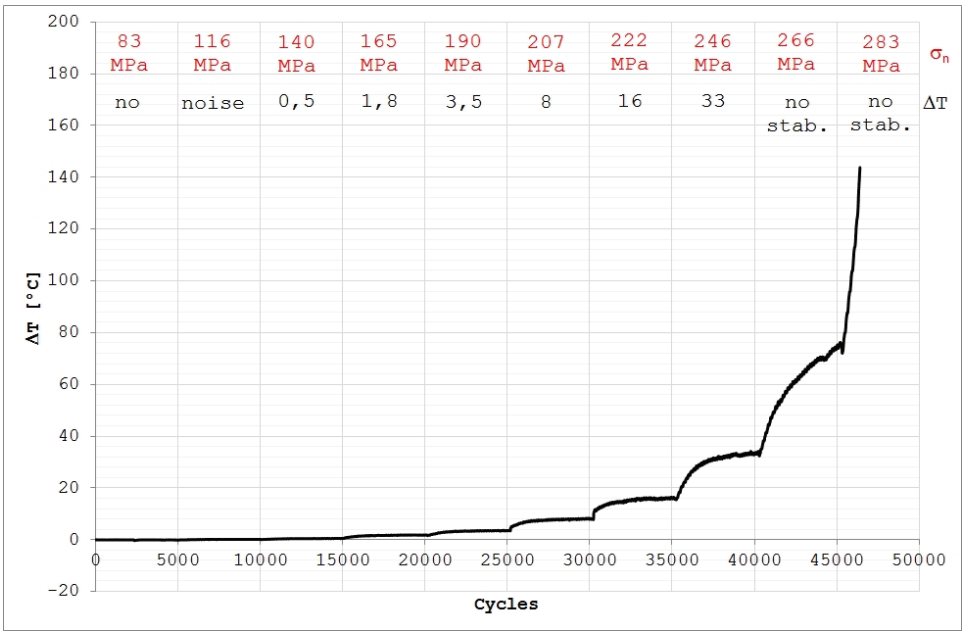

Figure 17: Average curve of temperature vs Cycles for different step loads.

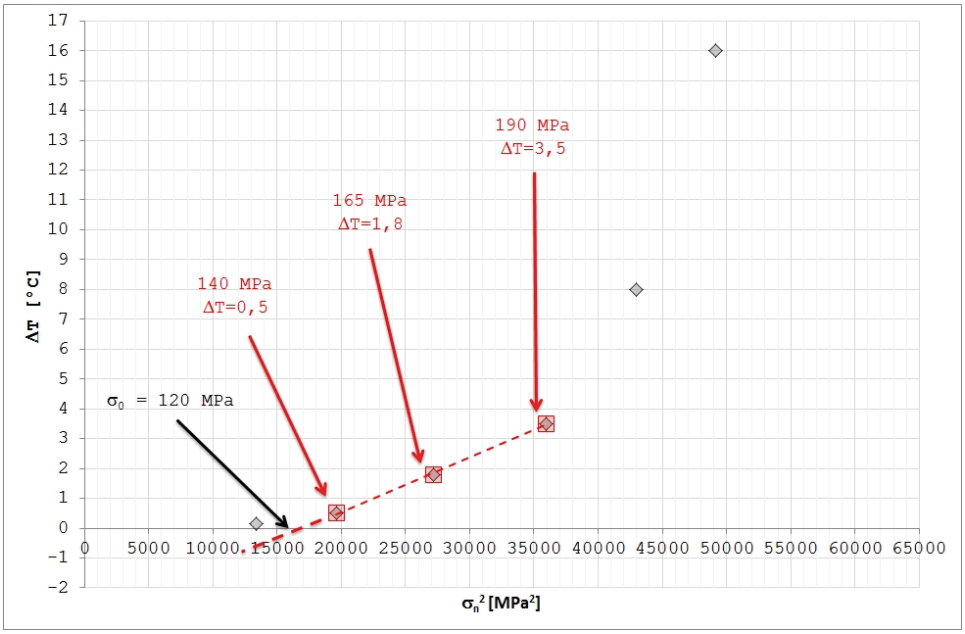

Figure 18: ΔT vs the applied stresses.

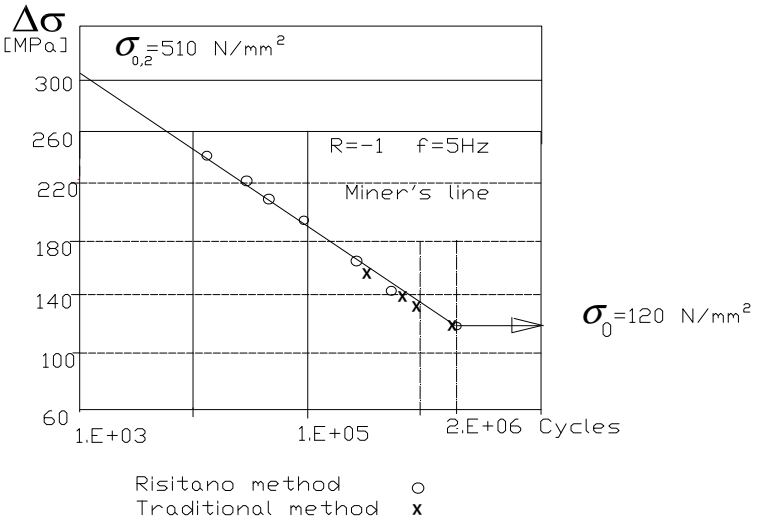

Figure 19: Wohler curve by Risitano method and traditional method.

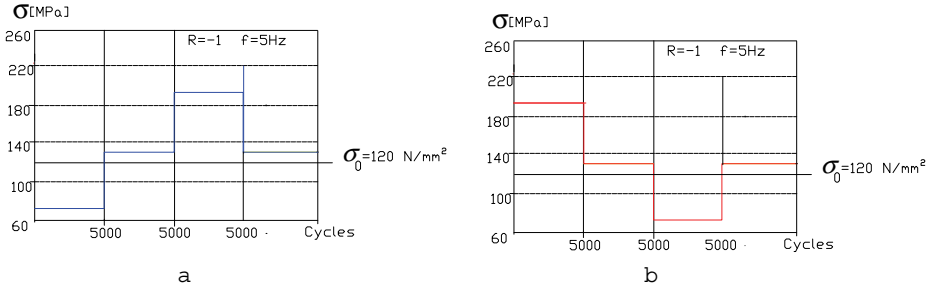

Figure 20: Equal applied loads in the two different sequences (A 20a, V 20b).

total value. Any value depends from the previous history as physically must be.

According to many authors, it is evident as the damage calculated by Miner's rule is underestimated in confrontation to the damage evaluated by mean of a method that put in account the energy lost in the previous fatigue cycles. It seem important to say as the energetic parameter $\int \Delta T \, dN$ used for the first time in Fargione, Geraci, La Rosa and Risitano (2002) as a material characteristic and, after, to define the damage ratio in Risitano A. and Risitano G. (2010) and (2011), is linked, in direct way, to the entropy γ of Nadery and Khonsary (2010) and to released Q of Atzori, Meneghetti and Ricotta (2009) that they use to evaluate the damage. All qualitative indications found for γ or Q are similar (the specific heat remains practically con-

stant) to these (in the past and now) used for the energetic parameter $\int \Delta T\, dn$ that, in equal and more direct way, is able to define the degradation of the material under fatigue process.

Table 4: Values of the damage calculated by the Miner's rule (D_M) and by the energy loosed (D_E) in the same cycles number.

Type A			Type V		
σ	r_M	r_E	ggσ	r_M	r_E
66	0,00	0,00	194	$4{,}75\text{x}10^{-2}$	$12{,}92\text{x}10^{-2}$
130	$0{,}36\text{x}10^{-2}$	$1{,}15\text{x}10^{-2}$	130	$0{,}36\text{x}10^{-2}$	$2{,}76\text{x}10^{-2}$
194	$4{,}75\text{x}10^{-2}$	$11{,}54\text{x}10^{-2}$	66	0,00	$0{,}77\text{x}10^{-2}$
130	$0{,}36\text{x}10^{-2}$	$3{,}08\text{x}10^{-2}$	130	$0{,}36\text{x}10^{-2}$	$3{,}38\text{x}10^{-2}$
66			194		
Total Damage for the equal applied loads	$5{,}47\text{x}10^{-2}$	$15{,}77\text{x}10^{-2}$		$5{,}47\text{x}10^{-2}$	$19{,}83\text{x}10^{-2}$

5 Conclusions

Following the rule of Miner, the fatigue life of a material or a mechanical component is not dependent on the order of load application. Many authors have already observed how the model proposed by Palmgren/Miner leads to an underestimation of the damage and one of the reasons may be that they did not consider the sequence of loads, path dependence, typical of irreversible phenomena. Referring to the energy loss related to the irreversible damage of the material, the authors in [Risitano A. and Risitano G. *JTAFM* (2010); Risitano A. and Risitano G. (2011)] have noted that the Miner rule does not lead to errors only if the damage caused by the fatiguing load is low compared to the limit energy of the material.

If instead the damage caused by the fatiguing load is high, Miner's rule is no longer valid and the greater the damage caused by loads previously applied the greater the error. In this paper, fatigue tests were performed with successive series of loads on a AISI 304 specimen. The load stories consisted of successive load ramps steps, the same blocks were applied to each group of specimens, but with reversed sequence of the ramps. So, an assessment of the specimen surface temperature was made, that as frequently aforementioned, represents an important parameter of the state of the specimen or of the mechanic component. It was confirmed that the value of the stabilization temperature $\Delta T2$ for damaged specimens does not depend only on applied load history, but also on the adopted sequence of loads. Indeed, the

succession of the load level is decisive for the damage generated to the material and a load history that changes between high and low loads is more " fatiguing " than a history with the same loads, but reversed (from low loads to high loads). The resulting residual life, estimated taking into consideration the temperature, as already mentioned in [Risitano A. and Risitano G. (2011)], would have different values. This is not detectable using the rule of Miner, even if it is valid and for some aspects (especially simplicity) convenient.

References

Atzori, B.; Meneghetti, G.; Ricotta, M. (2009): Analisi del comportamento a fatica a due livelli di carico di un acciaio inossidabile basata sulla dissipazione di energia, *XXXVIII AIAS*, Torino.

Corten, H. T.; Dolan, T. J. (1956): Cumulative Fatigue Damage, *Proc. of the International Conference on Fatigue of Metals*, Institute of Mechanical Engineers, London, pp. 235–245.

Curti, G.; La Rosa, G.; Orlando, M.; Risitano, A. (1986): Analisi Tramite Infrarosso Termico della Temperatura Limite in Prove di Fatica, *XIV AIAS*, Catania.

Di Schino, A.; Kenny, J.M. (2003): Grain size dependence of the fatigue behaviour of a ultrafine-grained AISI 304 stainless steel, Materials Letters, vol. 57, 21, pp. 3182-2185.

Fargione, G.; Geraci, A.; La Rosa, G.; Risitano, A. (2002): Rapid Determination of the Fatigue Curve by the Thermographic Method, *Int. J. Fatigue,* vol. 24, 1, pp. 11-19.

Fatemi, A.; Yang, L. (1998): Cumulative fatigue damage and life prediction theories: a survey of the state of the for homogeneus materials, *Int. J. Fatigue*, vol. 20, 1.

Haibach, E.: Modifizierte lineare Schadenakkumulationshypothese zur Berucksichtigung des Dauerfestigkeitsabfalls mit fortschreitender Schadigung, *Technische Mitteilungen* No. 50/70 der Lab. Fur Betriebsfestigkeit, Darmstadt, Germany.

Iqbal Rasool Memon; Xing Zhang; Deyu Cui (2002): Fatigue life prediction of 3-D problems by damage mechanics with two-block loading", *Int. J. Fatigue*, pp. 29–37.

La Rosa, G.; Risitano, A. (2000): Thermographic Methodology for Rapid Determination of the Fatigue Limit of Materials and Mechanical Components, *Int. J. Fatigue,* 22, pp. 65-73.

Lefebvre, D.; Ellyin, F. (1984): Cyclic response and inelastic strain energy in low cycle fatigue, *Int. J. Fatigue,* vol. 6, 1, pp. 9-15.

Manson, S. S.; Frecke, J. C.; Ensign, C. R. (1967): Applications of a Double Linear Damage Rule to Cumulative Fatigue, *Fatigue Crack Propagation, STP-415*, American Society for Testing and Materials, Philadelphia, p. 384.

Miner, M.A. (1945): Cumulative Damage in Fatigue, *Journal of Applied Mechanics*, 67, A159.

Naderi, M.; Amiri, M.; Khonsari, M.M. (2009): On the thermodynamic entropy of fatigue fracture, proceeding of the *Royal Society*.

Naderi, M.; Khonsary, M.M. (2010): A thermodynamic approach to fatigue damage accumulation under variable loading, *Matreials Science and Engeneering A*, 527, pp. 6133-6139.

Risitano, A.; Risitano, G. (2010): Analisi termica per la valutazione del comportamento a fatica di provini soggetti a successive serie di carichi, *Frattura ed Integrità Strutturale*, 12, pp. 88-99.

Risitano, A.; Risitano, G. (2010): Cumulate Damage Evaluation of Steel Using Infrared Thermography, *Journal Theoretical and Applied Fracture Mechanics*, vol. 54, 2, pp. 82-90.

Risitano, A.; Risitano, G. (2011): Cumulative Damage Model Using Analysis of Temperature Data Recorded During the Fatigue Test*, 13th International Conference Mesomechanics 2011*, Vicenza.

Palmgren, A. (1924): *Die Lebensdauer von Kugelgen*, Verfahrenstechnik, Berlin 68, 339.

Singh, A. (2001): An Experimental Investigation of Bending Fatigue Initiation and Propagation Lives, *J. Mech. Des.*, vol. 123, 3, pp.431-435.

Singh, A. (2002): The Nature of Initiation and Propagation S-N Curves and Below the Fatigue Limit, *Fatigue & Fracture of Engineering Materials & Structures*, vol.25, 1, pp. 79-89.